



Title	Poly(lactic acid/caprolactone) bilayer membrane achieves bone regeneration through a prolonged barrier function
Author(s)	Abe, Gabriela L.; Sasaki, Jun-Ichi; Tsuboi, Ririko et al.
Citation	Journal of Biomedical Materials Research - Part B Applied Biomaterials. 2024, 112(1), p. e35365
Version Type	AM
URL	https://hdl.handle.net/11094/93453
rights	© 2023 Wiley Periodicals LLC.
Note	

The University of Osaka Institutional Knowledge Archive : OUKA

<https://ir.library.osaka-u.ac.jp/>

The University of Osaka

Poly(lactic acid/caprolactone) bilayer membrane achieves bone regeneration through prolonged barrier function

Gabriela L Abe ^{1,2}, Jun-Ichi Sasaki ¹, Ririko Tsuboi ³, Tomoki Kohno ², Haruaki Kitagawa ^{1,2}, Satoshi Imazato ^{1,2}

¹ Department of Dental Biomaterials, Osaka University Graduate School of Dentistry, Suita, Osaka, Japan

² Joint Research Laboratory of Advanced Functional Materials Science, Osaka University Graduate School of Dentistry, Suita, Osaka, Japan

³ Department of Cariology, Restorative Sciences and Endodontics, University of Michigan School of Dentistry, Ann Arbor, Michigan, USA

Correspondence

Jun-Ichi Sasaki, Department of Dental Biomaterials, Osaka University Graduate School of Dentistry, 1-8 Yamadaoka, Suita, Osaka 565-0871, Japan.

Email: sasaki.junichi.dent@osaka-u.ac.jp

Funding information

Japan Society for the Promotion of Science, Grant/Award Numbers: 22K20989, 22H03952

Short running title

Barrier function of a polymeric membrane

Abstract

Guided bone regeneration (GBR) is a treatment strategy used to recover bone volume. Barrier membranes are a key component of GBR protocols, and their properties can impact treatment outcomes. This study investigated the efficacy of an experimental, slow-degrading, bilayer barrier membrane for application in GBR using in vivo animal models. A synthetic copolymer of poly(lactic acid/caprolactone) (PLCL) was used to prepare a slow-degrading bilayer membrane. The biodegradability of PLCL was evaluated by subcutaneous implantation in a rat model. The barrier function of the PLCL membrane was investigated in a rat calvaria defect model and compared with commercially available membranes composed of type I collagen (Col) and poly(lactic-co-glycolic acid) (PLGA). An alveolar bone defect model in beagle dogs was used to simulate GBR protocols to evaluate the bone regeneration ability of the experimental PLCL membrane. The PLCL membrane showed slow biodegradation, resulting in an efficient and prolonged barrier function compared with commercial materials. In turn, this barrier function enabled the space-making ability of PLCL membrane and facilitated bone regeneration. In the alveolar bone defect model, significantly greater regeneration was achieved by treatment with PLCL membrane compared with Col and PLGA membranes. Additionally, a continuous alveolar ridge contour was observed in PLCL-treated bone defects. In conclusion, the PLCL bilayer membrane is a promising biomaterial for use in GBR given its slow degradation and prolonged barrier function.

KEYWORDS

guided bone regeneration, barrier membrane, bilayer membrane, polylactic acid, polycaprolactone

1. INTRODUCTION

The presence of sufficient bone volume is correlated with a favorable prognosis for prosthetic rehabilitations, especially for dental implant treatments.^{1,2} Guided bone regeneration (GBR) uses surgical techniques and biomaterials to augment bone volume, thereby increasing the lifespan and overall aesthetics of dental implants and prostheses.³⁻⁵ The principle of GBR protocols is simple: to secure space for bone regeneration and prevent the invasion of connective or epithelial tissue into the bone defect area, allowing osteogenic cells to populate and regenerate the defective area.^{6,7} Thus, barrier membranes are a key element in GBR, functioning as a physical barrier against undesirable cells and tissues, and guarding the space for bone regeneration.⁸

Barrier membranes should show a defined degradation rate that is proportional and comparable to the local tissue regeneration.^{9,10} Bone regenerates slower than connective tissue, thus barrier membranes for GBR are required to function for an extended period. Non-degradable barrier membranes can be implemented, but they require a second surgery for retrieval;^{11,12} which can damage the regenerating tissue below, increasing the healing time, the procedural costs, and the burden to the patient. To address this issue, we have previously developed a slow-degrading barrier membrane for use in GBR composed of a copolymer of poly(lactic acid/caprolactone) (PLCL).^{13,14} Commercial biodegradable membranes were shown to suffer severe hydrolytic degradation within the first 3 months of water immersion, whereas the experimental PLCL membrane gradually degraded over a period of 12 months.¹⁴ Therefore, the experimental PLCL membrane with slower

degradation may provide a prolonged barrier function.

The structural design of the PLCL membrane also contributes to its functions. The membrane has a bilayer structure with a compact and a porous layer, where both layers are of the same composition but differ in morphology. The compact layer has a dense structure and smooth surface, providing an impenetrable barrier that was able to successfully block bacterial cells approximately one-tenth the size of epithelial cells.¹⁵ In contrast, the porous layer provides scaffold-like features, supporting cell proliferation and differentiation *in vitro*.¹⁴

In the present study, we investigated the experimental PLCL membrane using *in vivo* models that closely reproduce the clinical application of biomaterials. We hypothesized that the slow degradation combined with the bilayer design of the GBR membrane could provide a prolonged barrier function *in vivo*, leading to greater bone regeneration.

2. MATERIALS AND METHODS

2.1. Membrane preparation

The PLCL bilayer membrane was prepared as previously described.^{13,14} Briefly, PLCL was dissolved in 1,4-dioxane (Wako, Osaka, Japan), the copolymer solution was poured into a mold, and submitted to freeze-drying to obtain a porous film with an approximate thickness of 150 μm . A new solution of PLCL in 1,4-dioxane was prepared and poured into a second mold, and the previously obtained porous film was positioned directly over the new solution. The PLCL copolymer was allowed to dry at 60°C generating a compact and dense layer,

with an approximate thickness of 50 μm , at the bottom of the mold. This combined PLCL structure was cooled to room temperature and the resulting structure was a bilayer membrane with final thickness of 200 μm , composed of a compact layer and a porous layer. The bilayer membrane was sterilized by γ -radiation and stored at 4°C in a nitrogen atmosphere until use.

Two types of commercial biodegradable membranes were used as controls: a monolayer membrane composed of poly(lactic-co-glycolic acid) (PLGA) (GC membrane; GC, Tokyo, Japan) and a bilayer membrane composed of type I collagen (Col) (Bio-Gide; Geistlich Pharma AG, Wolhusen, Switzerland).

2.2. Subcutaneous biodegradation model

The protocol for evaluating biodegradation in a rat model was approved by the Ethical Committee of the American Association for Accreditation of Laboratory Animal Care (AAALAC) International (approval number: 17-070). To investigate the degradability of the PLCL membrane in a living tissue, membranes were implanted into the subcutaneous space of Fischer 344 (F344) rats. F344 rats were selected for their small size and ease of handling.

Nine-week-old male rats were housed in the Hamri Animal Unit (Hamri, Ibaraki, Japan), maintained in individual cages, and provided with water and pellet-type animal food ad libitum. For the surgical procedure, rats were anesthetized by inhalation of isoflurane gas (Mylan Seiyaku, Tokyo, Japan) at 2%–3% in pure oxygen as a carrier gas. Once adequate anesthesia was obtained, the dorsal hair was shaved off and povidone-iodine solution (Meiji

Seika Pharma, Tokyo, Japan) followed by 70% ethanol (Wako) was applied for disinfection of the back skin. An incision was made along the spine, then the skin and fascia were laterally displaced to create bilateral subcutaneous pouches. Four separate specimens of each membrane (10 × 10 mm) were implanted, two on each side of the animal, and the surgical area was closed with sutures. After 16 or 24 weeks, rats were euthanized using carbon dioxide, and then the membranes and the surrounding tissues were harvested ($n = 4$). Specimens were fixed using 10% neutral buffered formalin solution (Wako) for 24 h, embedded in paraffin, and sliced with a microtome (2125RT; Leica, Wetzlar, Germany) to obtain 5 μ m-thick sections. The sections were placed on a glass slide and deparaffinized followed by hematoxylin and eosin (HE) staining. A CCD camera (DS-Fi2; Nikon, Tokyo, Japan) attached to a light microscope (ECLIPSE CI-L; Nikon) was used for image capture.

2.3. Calvaria defect model

The protocol of the rat calvaria defect model was approved by the Institutional Animal Care and Use Committee of Graduate School of Dentistry (protocol number: 26-021-0).

Ten-week-old, male Sprague-Dawley rats (CLEA Japan, Tokyo, Japan) were used in this study. General anesthesia was performed using a mixture of three drugs: medetomidine (Domitor; Nippon Zenyaku Kogyo, Tokyo, Japan), midazolam (Dormicum; Maruishi Pharmaceutical, Osaka, Japan), and butorphanol (Vetorphale; Meiji Seika Pharma). The anesthetic solution contained 0.3 mg of medetomidine, 4.0 mg of midazolam, and 5.0 mg of

butorphanol per kilogram of body weight (bw). Saline was added to the mixture to achieve a working volume of 0.1 mL/10 g bw/animal, which was administered intra-peritoneally.¹⁶

After anesthesia, the top of the head was shaved, and a flap was raised to expose the calvarium. The periosteum was laterally displaced and carefully preserved. A standardized 5-mm diameter trephine bur (Micro Tech, Tokyo, Japan) was used to prepare bone defects at the left and right parietal bones. Barrier membranes were trimmed to a circular shape with a 7-mm diameter to completely cover the defect area. According to randomly assigned experimental groups, barrier membranes were applied in position to cover each defect area. For positioning the commercial membranes, the manufacturer's instructions were followed; for positioning the PLCL membrane, the compact layer faced the periosteum, and the porous layer faced the bone defect. Subsequently, the periosteum was repositioned and closed with an absorbable suture (Vicryl 6-0; Ethicon, Bridgewater, NJ, USA), and the dermis was closed with a non-absorbable suture (Nescosuture 4-0; Alfresa Pharma, Osaka, Japan). Calvaria were harvested at 4 weeks post-surgery ($n = 3$) or 8 weeks post-surgery ($n = 5$).

2.4. Alveolar bone defect GBR model

The protocol for the dog alveolar bone defect model was approved by the AAALAC International (approval number: 13-H065). Male beagle dogs (weight: 8–11 kg) were obtained from Kitayama Labes (Nagano, Japan) and housed in individual cages under a controlled environment in the Hamri Animal Unit (Hamri). Beagle dogs were provided with water and pellet-type animal food ad

libitum.

The anesthetic solution contained equal amounts of ketamine hydrochloride (Ketalar; Daiichi Sankyo Propharma, Tokyo, Japan) and xylazine (Ceractal; Bayer, Leverkusen, Germany) and was administered at 0.4 mL/kg bw/animal via intramuscular injection. In addition, a subgingival injection of lidocaine (Dentsply-Sirona, Tokyo, Japan) was administered to the surgical site for local anesthesia. Before the operation, enrofloxacin (Baytril; Bayer, Leverkusen, Germany) at 10 mg/kg bw was administered intramuscularly to prevent infections, and the surgical site was disinfected with povidone-iodine solution (Meiji Seika Pharma).

The fourth mandibular premolar (P4) was extracted, and a buccal dehiscence-type cavity was formed in the P4 socket using a micromotor unit (Vivamate G5; Nakanishi, Tochigi, Japan) and a fissure bur (Morita, Suita, Japan). The final bone defect prepared had an anteroposterior length of 10 mm, a depth of 5 mm, and a buccolingual width of 4 mm. Next, a bone substitute material (Cytrans Granules; GC) was applied to fill in the bone defect area and the different barrier membranes were used to cover the defect. Four experimental conditions were established: sham treatment, using bone substitute material only; PLGA treatment, using bone substitute and PLGA membrane; PLCL treatment, using bone substitute and PLCL membrane; and Col treatment, using bone substitute and Col-based membrane ($n = 4$). Finally, the flaps were repositioned and the gingiva was closed with 4-0 nylon sutures. Buprenorphine (Lepetan; Otsuka Pharmaceutical, Tokushima, Japan) was subcutaneously administered at 20 μ g/kg bw for pain relief once a day for

4 days. Twelve weeks after implantation, the animals were euthanized, and mandibles were collected for micro-computed tomography (micro-CT) observation and histological analysis.

2.5. Micro-CT and histological evaluation

To quantify the newly formed bone in the rat and dog models, retrieved samples were scanned by micro-CT (R_mCT2; Rigaku, Tokyo, Japan) with a 20 × 20 mm scan field of view and 40 μm resolution. Bone areas were identified using the density values of a hydroxyapatite phantom control (200–800 mg/cm³) as reference. The volume ratio of regenerated bone in relation to the defect site was determined using image analysis software (TRI/3D-BON; RATOC, Tokyo, Japan) as previously described.¹⁷

Histological evaluation of newly formed bone was performed after the micro-CT scanning. Specimens were fixed by neutral buffered formalin solution (Wako), then decalcified using Morse solution (Wako) for 2–6 days until adequate decalcification was achieved. Specimens were embedded in paraffin using an automatic paraffin-embedding device (CT-Pro20; Genostaff, Tokyo, Japan) and sliced into 5-μm thick sections using a microtome (2125RT). For observation, HE staining and Masson-Goldner staining were performed, and a light microscope (ECLIPSE CI-L) coupled with a CCD camera (DS-Fi2) was used for image capture. Masson-Goldner staining indicates the state of bone maturation; newly synthesized bone matrix appears as green and mineralized mature bone appears as red. Additionally, images were captured with polarized light to further distinguish host tissues from the remaining structures of the

barrier membranes.

2.6. Statistical analysis

The two-way analysis of variance (ANOVA) was used, and a significant difference was defined as a value of $p < 0.05$. The graphical representation of this analysis shows the mean and standard deviation bars.

3. RESULTS

3.1. Biodegradation of the barrier membrane

Biodegradation of the membranes in the rat subcutaneous space is shown in Figure 1. PLGA membrane showed severe degradation at week 16, and remnants of the membrane structure were entirely infiltrated by host cells (Figure 1A). Col membrane was not found in the tissue at week 16 after implantation, indicating complete degradation by the host (Figure 1B). Conversely, PLCL membrane prevented cell infiltration through the compact layer, which resulted in the formation of a cell lining directly above this layer (Figure 1C). The porous layer showed partial infiltration by host cells, acting as a scaffold for the cells in direct contact.

After 24 weeks, PLGA and Col membranes were completely degraded (Figure 1D,E). PLCL membrane showed progressive degradation while maintaining the bilayer structure (Figure 1F). The porous layer of the PLCL membrane showed greater cell infiltration compared with that at week 16, however, the compact layer maintained a clear separation from the host cells. These results indicated that PLCL membrane maintained an efficient barrier

function, as well as providing a scaffold, after 24 weeks of implantation.

3.2. Bone regeneration in calvaria defect model

Micro-CT images of the parietal bones of rats showed that all membranes supported bone regeneration (Figure 2A). No significant differences were observed in the volume of newly formed bone relative to the defect size among the three groups at week 4 (Figure 2B). After 8 weeks, all treatments showed an average bone regeneration of over 50% of the original defect area, and PLCL membrane group showed significantly greater bone regeneration ($71.8\% \pm 14.6\%$) in comparison with PLGA and Col membrane groups (Figure 2B).

The histological observations of regenerated bone at week 4 are shown in Figure 3A,B. All membranes showed cell infiltration allowing for bone regeneration; however, only PLGA and PLCL membranes showed a barrier function against soft tissue. Col membrane was completely populated by host cells and acted as a scaffold but not as a barrier. The magnified images in Figure 3B show that the degradation of PLGA membrane was accompanied by cell invasion into the membrane structure. Col membrane was indistinguishable from the host soft tissue and entirely populated by host cells. PLCL membrane showed initial degradation of the porous layer with cell infiltration, however, the compact layer showed a cell lining directly in contact with the membrane surface but no cell infiltration.

Figure 3C,D shows HE staining of the calvaria at week 8. Treatment with PLGA membrane resulted in uneven bone formation with severe degradation of the membrane and complete infiltration by host cells. Col membrane had

collapsed into the bone defect, creating a concavity, and reducing the vertical space for bone regeneration. As a result, thinner bone formation was observed after Col membrane treatment compared with PLGA and PLCL membranes. PLCL membrane maintained the bilayer structure, which showed further degradation of the porous layer and infiltration by host cells on the bone defect side. However, the compact layer of PLCL membrane preserved its barrier function against cell infiltration (Figure 3D).

Bone regeneration in the rat calvaria defect model was evaluated by Masson-Goldner staining (Figure 4), which allows visualization of the bone maturation by distinguishing between newly synthesized bone matrix, which appears green, and mineralized mature bone, which appears red. The panoramic view shows bone regeneration with mineralized mature bone for all treatments without the presence of fibrosis; however, PLCL and Col treatments resulted in greater maturation than observed for the defects treated with PLGA (Figure 4A). In the magnified view, new bone matrix deposition could be seen for all treatments, and mature bone could be observed in direct contact with PLCL and PLGA membranes, (Figure 4B). The residual membranes were observed under polarized light (Figure 4C), which indicated that the bilayer structure of the PLCL membrane was preserved; however, PLGA membrane showed advanced degradation and Col membrane was completely degraded, at 8 weeks post-surgery. Therefore, the prolonged barrier function of PLCL membrane provided the required space and promoted bone regeneration in the calvaria defect model.

3.3. Tissue regeneration in the GBR model

To evaluate the behavior of the experimental PLCL bilayer membrane in a GBR model that closely reproduces the clinical situation, a standardized bone defect was prepared in the mandible of beagle dogs. Figure 5A shows micro-CT images of the surgical site after 12 weeks of implantation. All the bone defects were partially regenerated, including in the sham-treatment group where no barrier membrane was used. Bone defects treated with PLCL membrane showed a continuous and regular alveolar ridge contour compared with defects treated with control membranes. PLGA and Col membrane treated defects exhibited an uneven and irregular alveolar ridge contour, which was similar to that of sham-treated defects. Quantitative analysis revealed that PLCL membrane had significantly greater tissue regeneration, including marrow and cortical bone regeneration, compared with sham and control treatments (Figure 5B). These differences may be attributed to the prolonged barrier function of PLCL membrane, which prevented the infiltration of connective and epithelial tissues into the defect area.

The histological images at 12 weeks after surgery are shown in Figure 5C. The defects treated with bone substitutes and PLCL membrane showed greater replacement of the substitute material with bone marrow and cortical bone. Bone substitutes were observed surrounded by fibrous tissue in the defects treated with control membranes or sham treatment. This observation indicated that invading cells from the surrounding soft tissues may have deposited fibrous tissue, which in turn restricted the replacement of bone substitutes for new bone.

4. DISCUSSION

Barrier membranes are key biomaterials for GBR protocols because of their ability to secure the space for bone regeneration and allow osteogenic cells to regenerate within the bone defect. In the present study, a PLCL membrane with a bilayer structure displayed an efficient barrier function in vivo and promoted bone regeneration with a favorable alveolar ridge contour in a GBR experimental model.

Increasing the time to degradation of barrier membranes has been attempted in several studies.^{18–20} The strategies differed depending on the base material for membrane fabrication, and cross-linking and copolymerization were the two most common strategies.²¹ Cross-linked membranes often show decreased degradation rates but are accompanied by cytotoxic effects caused by the cross-linking agents, raising concerns regarding the higher rates of postoperative complications, compared with other membranes.^{19,20} Copolymerized synthetic polymers are considerably less toxic because medical grade polymers can be hydrolyzed in the body and the degradation products can be excreted by several mechanisms.^{22,23} The degradation rate of PLCL membrane obtained via the copolymerization of biodegradable polymers used in the present study has been previously analyzed,^{13–15} and herein we showed that the slow degradation of this biomaterial resulted in an extension of the barrier function.

The subcutaneous implantation model was used to elucidate two different properties of the PLCL membrane, which are directly related to the bilayer

structure. The compact layer provided an efficient barrier, creating a clear interface between the membrane and the host tissue, with cells adhered to the surface of this layer but with no cell invasion. The porous layer allowed cell infiltration and performed a scaffold-like role, providing three-dimensional support for cell adhesion and proliferation. PLGA and Col membranes did not show barrier behavior; these membrane structures were thoroughly populated by host cells and were completely degraded by 24 weeks. The behavior of the control membranes was more suggestive of a scaffold than of a barrier membrane.^{24,25} Although, PLGA membrane could be considered to have acted as a barrier for at least 4 weeks.

The quantification of regenerated bone in the rat calvaria defect model showed that all membranes promoted bone regeneration; however, histological observations revealed that only PLCL membrane had an intact structure and provided a barrier against connective and epithelial tissues. In particular, PLCL membrane had a greater volume ratio of regenerated bone, compared with Col membrane, a material expected to show bioactive properties.^{26,27} The bioactive properties of several collagen-based membranes are assumed to be derived from their ability to induce cytokine production in local cells, subsequently creating a microenvironment conducive to cellular proliferation and differentiation.^{28,29} Regardless of its bioactivity, Col membrane showed a lack of space-making ability but still acted as a scaffold, and the results reported here agree with previous reports.²⁹⁻³¹ These results can also be discussed with regards to the differences in structure and composition among the barrier membranes. Col membrane presents a mesh-like structure, hydrophilic and

permeable in aqueous environments, allowing greater cell infiltration.^{14,15} PLGA shows interconnected pores that also allow cell infiltration, however the hydrophobic nature of this material may slow down permeability. PLCL is characterized by wide pores that permitted cells to infiltrate the porous layer,¹⁴ though the presence of a compact layer in direct contact with the surgical flap prevented epithelial cell invasion of the bone defect. In essence, bone regeneration is strongly dependent on osteogenic cells to produce bone matrix, and invading epithelial or soft tissue cells disturb the process of regeneration leading to fibrosis.^{32,33}

Considering the mechanical properties of biodegradable barrier membranes in comparison with non-degradable membranes, studies have recommended that bone-substitute materials are used in conjunction with biodegradable membranes to provide physical support and prevent collapse.^{34,35} In the in vivo GBR model, a carbonate apatite bone substitute with demonstrated osteoconductivity was used.^{36,37} Defects treated with bone substitute and PLCL membrane had significantly greater regeneration than those treated with bone substitute and PLGA or Col membranes. This result indicated that, even though membrane collapse can be prevented by the use of bone grafting materials, the efficient barrier function of PLCL membrane against invading cells further promoted regeneration, compared with the other membranes. Furthermore, the PLCL membrane may have contributed to the formation of a regular and continuous alveolar ridge contour in the defects treated with this biomaterial.

5. CONCLUSION

The slow-degrading bilayer PLCL membrane showed prolonged functions, compared with other tested membranes. The compact layer was responsible for efficiently blocking undesirable cells from invading bone defects, while the porous layer performed a scaffold-like role, supporting cell adhesion and proliferation. These properties resulted in greater bone regeneration for defects treated with PLCL membrane, compared with those treated with commercial Col or PLGA membranes. Overall, it was demonstrated that the PLCL bilayer membrane is useful for GBR applications.

AUTHOR CONTRIBUTIONS

Gabriela L Abe: Investigation, Formal analysis, Validation, Data Curation, Writing – original draft, Visualization, Funding acquisition. Jun-Ichi Sasaki: Conceptualization, Methodology, Project administration, Writing – original draft, Funding acquisition. Ririko Tsuboi: Investigation, Methodology. Tomoki Kohno: Investigation, Resources. Haruaki Kitagawa: Investigation, Writing – review & editing. Satoshi Imazato: Conceptualization, Project administration, Supervision, Writing – review & editing.

ACKNOWLEDGEMENTS

This work was supported by Grants-in-Aid for Scientific Research (22K20989 to G.L. Abe and 22H03952 to J.I. Sasaki) from the Japan Society for the Promotion of Science.

CONFLICT OF INTEREST STATEMENT

The authors declare no conflicts of interest.

DATA AVAILABILITY STATEMENT

The data that support the findings of this study are available from the corresponding author upon reasonable request.

REFERENCES

1. Elgali I, Omar O, Dahlin C, Thomsen P. Guided bone regeneration: materials and biological mechanisms revisited. *Eur J Oral Sci.* 2017;125(5):315–337.
2. Behring J, Junker R, Walboomers XF, Chessnut B, Jansen JA. Toward guided tissue and bone regeneration: morphology, attachment, proliferation, and migration of cells cultured on collagen barrier membranes. A systematic review. *Odontology.* 2008;96:1–11.
3. Fiorellini JP, Nevins ML. Localized ridge augmentation/preservation. A systematic review. *Ann Periodontol.* 2003;8(1):321–327.
4. Faria-Almeida R, Astramskaite-Januseviciene I, Puisys A, Correia F. Extraction socket preservation with or without membranes, soft tissue influence on post extraction alveolar ridge preservation: a systematic review. *J Oral Maxillofac Res.* 2019;10(3):e5.
5. Masquelet AC, Begue T. The concept of induced membrane for reconstruction of long bone defects. *Orthop Clin North Am.* 2010;41(1):27–37.
6. Hoornaert A, d'Arros C, Heymann MF, Layrolle P. Biocompatibility, resorption and biofunctionality of a new synthetic biodegradable membrane for guided bone regeneration. *Biomed Mater.* 2016;11(4):045012.
7. Liu J, Kerns DG. Mechanisms of guided bone regeneration: a review. *Open Dent J.* 2014;8:56–65.
8. Polimeni G, Xiropaidis AV, Wikesjö UME. Biology and principles of periodontal wound healing/regeneration. *Periodontol 2000.* 2006;41(1):30–47.
9. Wang J, Wang L, Zhou Z, Lai H, Xu P, Liao L, et al. Biodegradable polymer membranes applied in guided bone/tissue regeneration: a review. *Polymers.* 2016;8(4):115.
10. Ren Y, Fan L, Alkildani S, Liu L, Emmert S, Najman S, et al. Barrier membranes for guided bone regeneration (GBR): a focus on recent advances in collagen membranes. *Int J Mol Sci.* 2022;23(23):14987.
11. Sasaki JI, Abe GL, Li A, Thongthai P, Tsuboi R, Kohno T, et al. Barrier membranes for tissue regeneration in dentistry. *Biomater Investig Dent.* 2021;8(1):54–63.
12. Bee SL, Hamid ZAA. Asymmetric resorbable-based dental barrier membrane for periodontal guided tissue regeneration and guided bone

- regeneration: a review. *J Biomed Mater Res Part B Appl Biomater*. 2022;110(9):2157–2182.
13. Yoshimoto I, Sasaki JI, Tsuboi R, Yamaguchi S, Kitagawa H, Imazato S. Development of layered PLGA membranes for periodontal tissue regeneration. *Dent Mater*. 2018;34(3):538–550.
 14. Abe GL, Sasaki JI, Katata C, Kohno T, Tsuboi R, Kitagawa H, et al. Fabrication of novel poly(lactic acid/caprolactone) bilayer membrane for GBR application. *Dent Mater*. 2020;36(5):626–634.
 15. Abe GL, Tsuboi R, Kitagawa H, Sasaki JI, Li A, Kohno T, et al. Poly(lactic acid/caprolactone) bilayer membrane blocks bacterial penetration. *J Periodontal Res*. 2022;57(3):510–518.
 16. Kirihaara Y, Takechi M, Kurosaki K, Kobayashi Y, Kurosawa T. Anesthetic effects of a mixture of medetomidine, midazolam and butorphanol in two strains of mice. *Exp Anim*. 2013;62(3):173–180.
 17. Tsuboi R, Sasaki JI, Kitagawa H, Yoshimoto I, Takeshige F, Imazato S. Development of a novel dental resin cement incorporating FGF-2-loaded polymer particles with the ability to promote tissue regeneration. *Dent Mater*. 2018;34(4):641–648.
 18. Florjanski W, Orzeszek S, Olchowy A, Grychowska N, Wieckiewicz W, Malysa A, et al. Modifications of polymeric membranes used in guided tissue and bone regeneration. *Polymers*. 2019;11(5):782.
 19. Wu Y, Chen S, Luo P, Deng S, Shan Z, Fang J, et al. Optimizing the biodegradability and biocompatibility of a biogenic collagen membrane through cross-linking and zinc-doped hydroxyapatite. *Acta Biomater*. 2022;143:159–172.
 20. Veríssimo DM, Leitão RFC, Ribeiro RA, Figueiró SD, Sombra AS, Góes JC, et al. Polyanionic collagen membranes for guided tissue regeneration: effect of progressive glutaraldehyde cross-linking on biocompatibility and degradation. *Acta Biomater*. 2010;6(10):4011–4018.
 21. Jiménez Garcia J, Berghezán S, Caramês JMM, Dard MM, Marques DN. Effect of cross-linked vs non-cross-linked collagen membranes on bone: a systematic review. *J Periodontal Res*. 2017;52(6):955–964.
 22. Huang MH, Li S, Hutmacher DW, Coudane J, Vert M. Degradation characteristics of poly(ϵ -caprolactone)-based copolymers and blends. *J Appl Polym Sci*. 2006;102(2):1681–1687.
 23. Lam CXF, Savalani MM, Teoh SH, Hutmacher DW. Dynamics of in vitro

polymer degradation of polycaprolactone-based scaffolds: accelerated versus simulated physiological conditions. *Biomed Mater*. 2008;3(3):034108.

24. Gao Y, Wang S, Shi B, Wang Y, Chen Y, Wang X, et al. Advances in modification methods based on biodegradable membranes in guided bone/tissue regeneration: a review. *Polymers*. 2022;14(5):871.
25. Turri A, Elgali I, Vazirisani F, Johansson A, Emanuelsson L, Dahlin C, et al. Guided bone regeneration is promoted by the molecular events in the membrane compartment. *Biomaterials*. 2016;84:167–183.
26. Lindner C, Alkildani S, Stojanovic S, Najman S, Jung O, Barbeck M. In vivo biocompatibility analysis of a novel barrier membrane based on bovine dermis-derived collagen for guided bone regeneration (GBR). *Membranes*. 2022;12(4):378.
27. Liu Z, Wei P, Cui Q, Mu Y, Zhao Y, Deng J, et al. Guided bone regeneration with extracellular matrix scaffold of small intestinal submucosa membrane. *J Biomater Appl*. 2022;37(5):805–813.
28. Kanematsu A, Marui A, Yamamoto S, Ozeki M, Hirano Y, Yamamoto M, et al. Type I collagen can function as a reservoir of basic fibroblast growth factor. *J Control Release*. 2004;99(2):281–292.
29. Calciolari E, Ravanetti F, Strange A, Mardas N, Bozec L, Cacchioli A, et al. Degradation pattern of a porcine collagen membrane in an in vivo model of guided bone regeneration. *J Periodontal Res*. 2018;53(3):430–439.
30. Retzepi M, Donos N. Guided bone regeneration: biological principle and therapeutic applications. *Clin Oral Implants Res*. 2010;21(6):567–576.
31. Iviglia G, Kargozar S, Baino F. Biomaterials, current strategies, and novel nano-technological approaches for periodontal regeneration. *J Funct Biomater*. 2019;10(1):3.
32. Sanz M, Dahlin C, Apatzidou D, Artzi Z, Bozic D, Calciolari E, et al. Biomaterials and regenerative technologies used in bone regeneration in the craniomaxillofacial region: consensus report of group 2 of the 15th European Workshop on Periodontology on Bone Regeneration. *J Clin Periodontol*. 2019;46(Suppl 21):82–91.
33. Cucchi A, Chierico A, Fontana F, Mazzocco F, Cinquegrana C, Belleggia F, et al. Statements and recommendations for guided bone regeneration: consensus report of the Guided Bone Regeneration Symposium held in Bologna, October 15 to 16, 2016. *Implant Dent*. 2016;28(4):388–399.

34. van Oirschot B, Mikos AG, Liu Q, van den Beucken JJ, Jansen JA. Fast degradable calcium phosphate cement for maxillofacial bone regeneration. *Tissue Eng Part A*. 2023;29(5–6):161–171.
35. Zampara E, Alshammari M, De Bortoli J, Mullings O, Gkissakis IG, Benalcázar Jalkh EB, et al. A histological and histomorphometric evaluation of an allograft, xenograft, and alloplast graft for alveolar ridge preservation: randomized clinical trial. *J Oral Implantol*. 2022;48(6):541–549.
36. Ishikawa K, Miyamoto Y, Tsuchiya A, Hayashi K, Tsuru K, Ohe G. Physical and histological comparison of hydroxyapatite, carbonate apatite, and β -tricalcium phosphate bone substitutes. *Materials*. 2018;11(10):1993.
37. Mano T, Akita K, Fukuda N, Kamada K, Kurio N, Ishikawa K, et al. Histological comparison of three apatitic bone substitutes with different carbonate contents in alveolar bone defects in a beagle mandible with simultaneous implant installation. *J Biomed Mater Res B Appl Biomater*. 2020;108(4):1450–1459.

Figure legends

FIGURE 1 Histological images of the subcutaneous degradation of membranes stained by HE. (A, D) PLGA, (B, E) Col, and (C, F) PLCL at (A–C) week 16 and (D–E) week 24. Black arrowheads indicate the limits of implanted membranes. Scale bars: 100 μ m.

FIGURE 2 (A) Micro-CT images of rat calvaria at 4- and 8-weeks post-surgery. Scale bars: 1 mm. (B) Volume ratios of regenerated bone calculated for each experimental condition. The same letters indicate there was no significant difference between experimental conditions ($p < 0.05$, mean \pm SD).

FIGURE 3 Histological images of rat calvaria stained by HE at (A, B) 4 weeks and (C, D) 8 weeks post-surgery. (A, C) Cross-section of bone defects and (B, D) magnified images. Black arrowheads indicate the limits of calvaria defects. Empty arrowheads indicate cell linings in contact with the PLCL compact layer. Scale bars: (A, C) 1 mm; (B, D) 100 μ m. m: membrane; rb: regenerated bone; st: soft tissue; cc: cranial cavity.

FIGURE 4 Histological images of rat calvaria stained by Masson-Goldner at 8 weeks post-surgery. Black arrowheads indicate the limits of calvaria defects. Asterisks indicate newly deposited bone matrices. m: membrane; cc: cranial cavity. Scale bars: (A) 1 mm; (B, C) 100 μ m.

FIGURE 5 Alveolar bone defects treated with barrier membranes and bone substitutes at 12 weeks post-surgery. (A) Micro-CT images of the surgical site. (B) Volume ratios of regenerated tissue and bone substitutes for each experimental condition. (C) Histological images of treated bone defects stained by HE. Scale bars: (A, B) 2 mm, * $p < 0.05$, mean \pm SD.

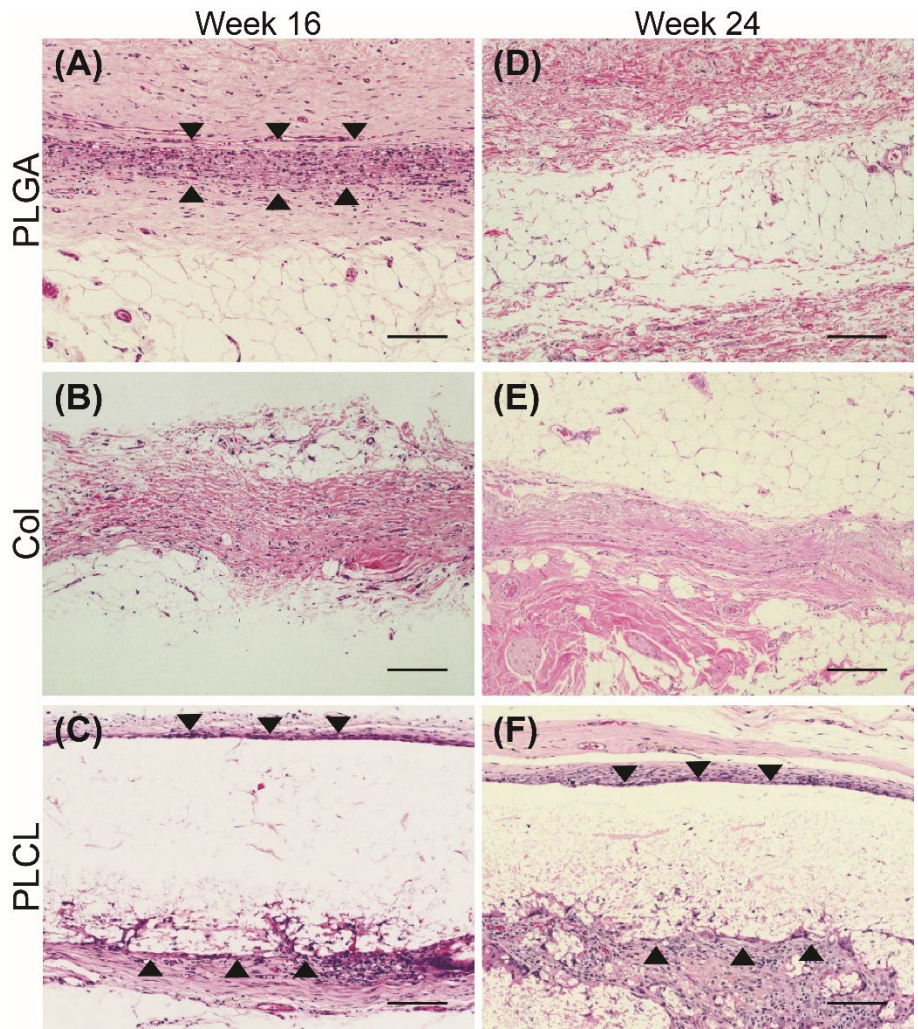


FIGURE 1

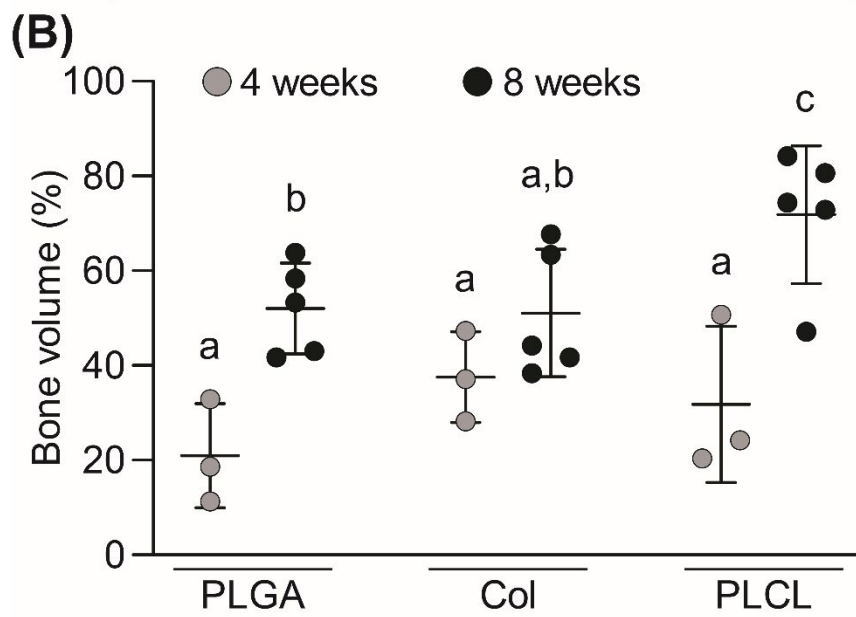
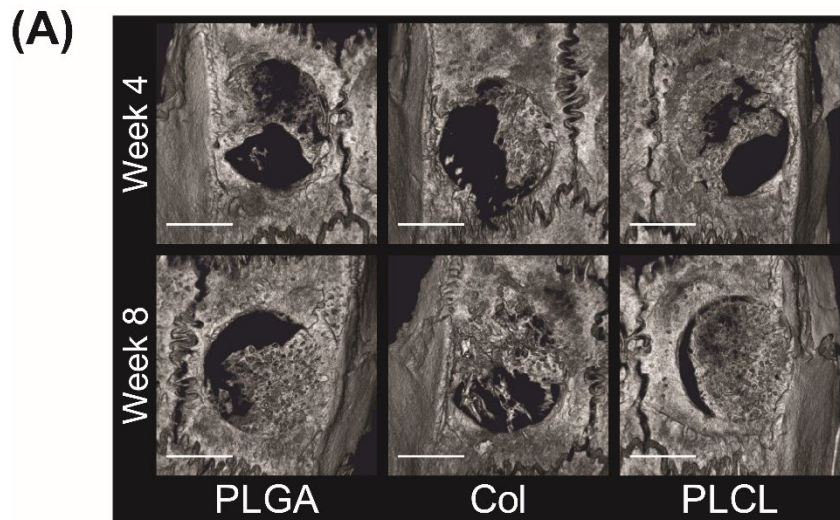


FIGURE 2

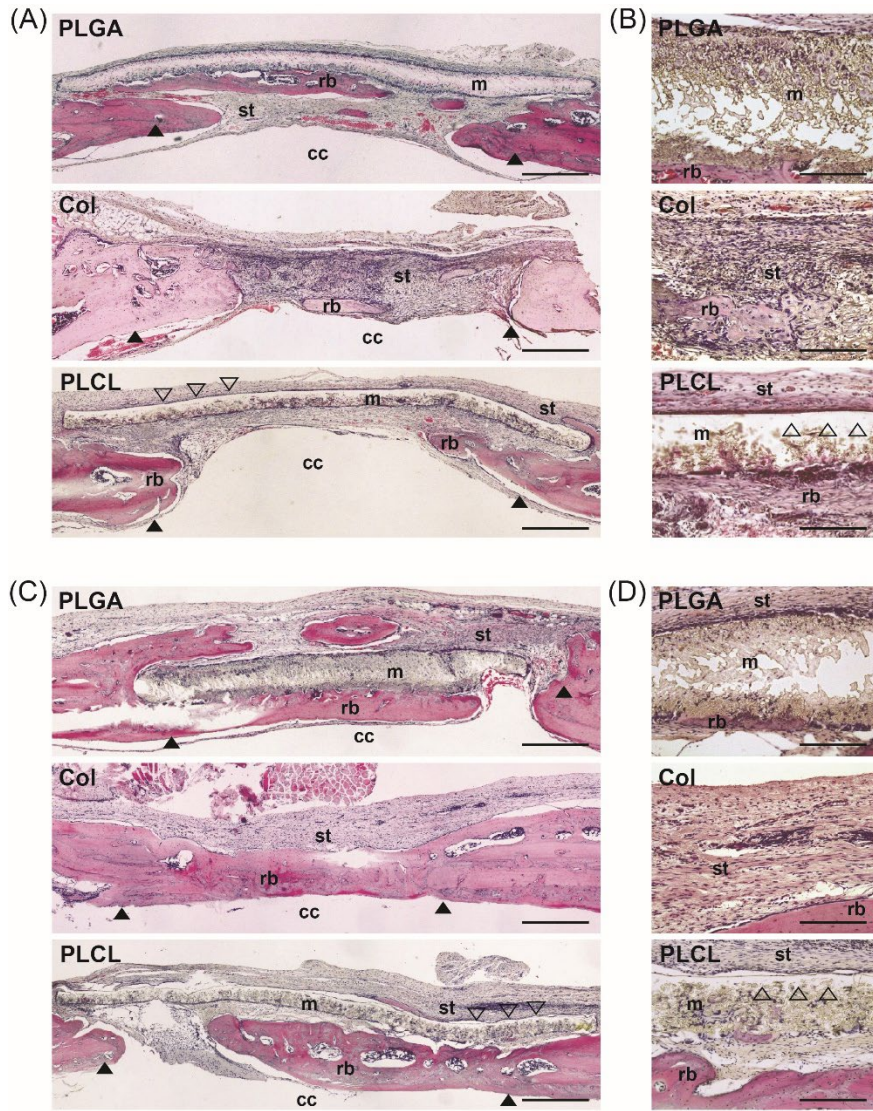


FIGURE 3

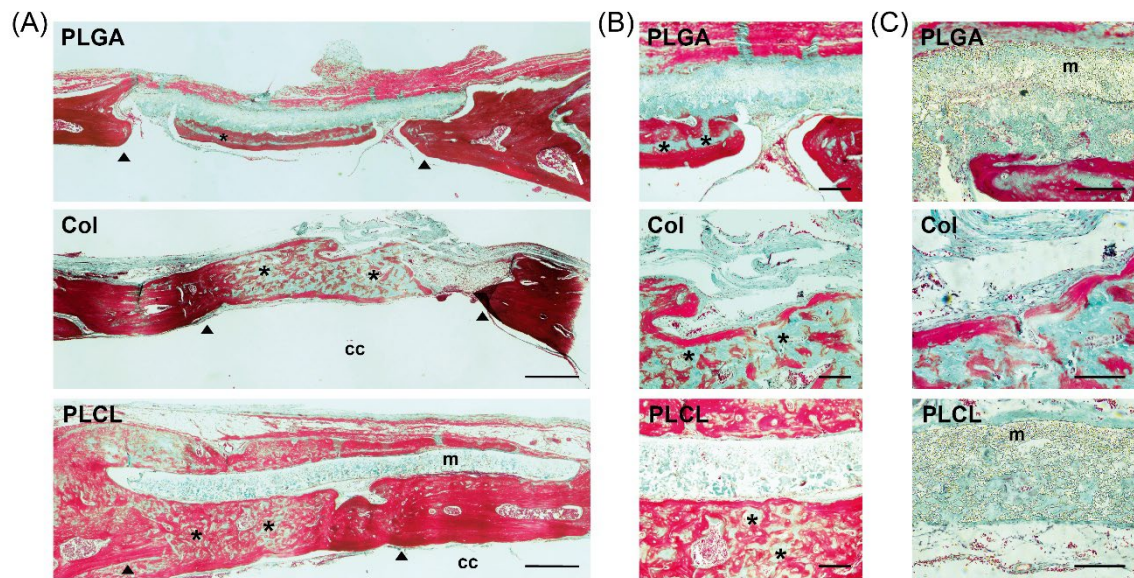


FIGURE 4

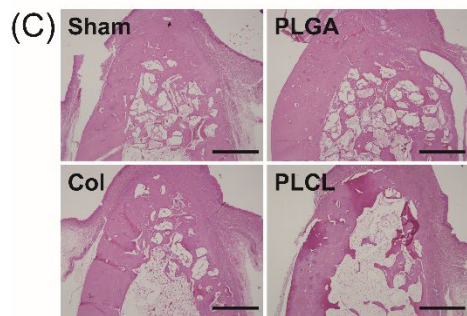
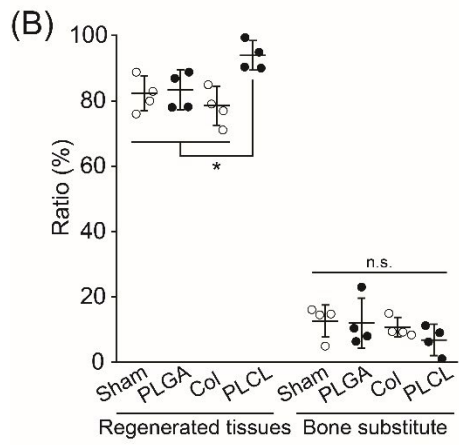
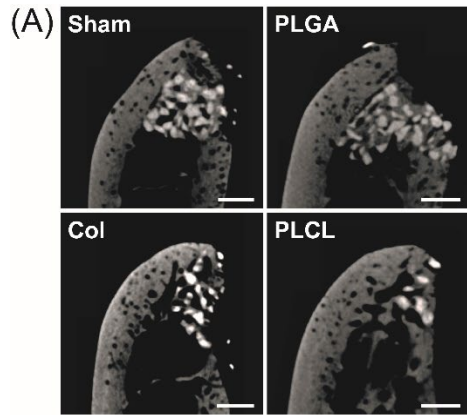


FIGURE 5